Electronic Supplementary Material (ESI) for Physical Chemistry Chemical Physics.

Supporting Information

Trion dynamics and charge photogeneration in MoS_2 nanosheets prepared by liquid phase exfoliation

Yuan-Yuan Yue,[†] Le-Yi Zhao,[†] Dan-Ao Han,[†] Lei Wang,*[,†] Hai-Yu Wang,*[,†] Bing-Rong Gao,[†] and Hong-Bo Sun[‡]

[†]State Key Laboratory of Integrated Optoelectronics, College of Electronic Science and Engineering, Jilin University, 2699 Qianjin Street, Changchun 130012, China.
[‡]State Key Laboratory of Precision Measurement Technology and Instruments, Department of Precision Instrument, Tsinghua University, Haidian, Beijing 100084, China.

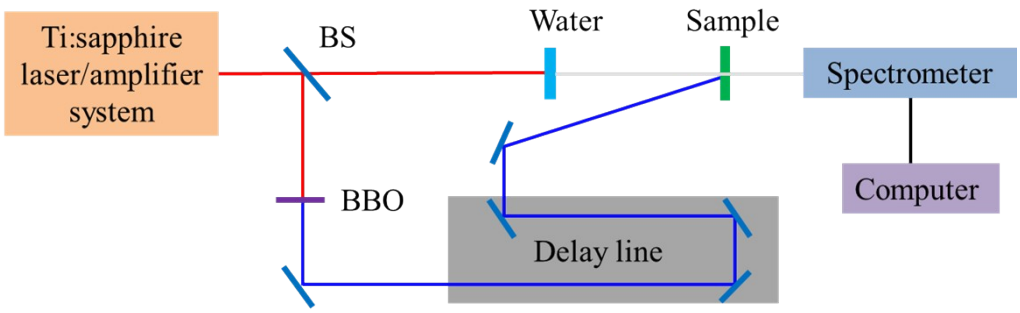

Figure S1. The schematic of femtosecond transient absorption setup.

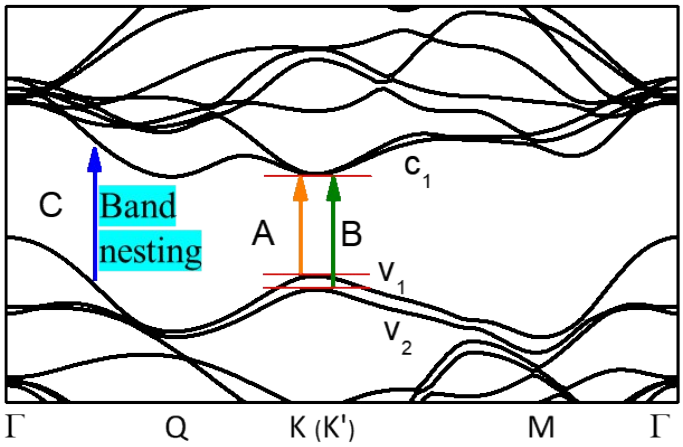

Figure S2. The schematic of multilayer MoS_2 band structure. The band-nesting nature of C-exciton state still calls for deep investigations in future.

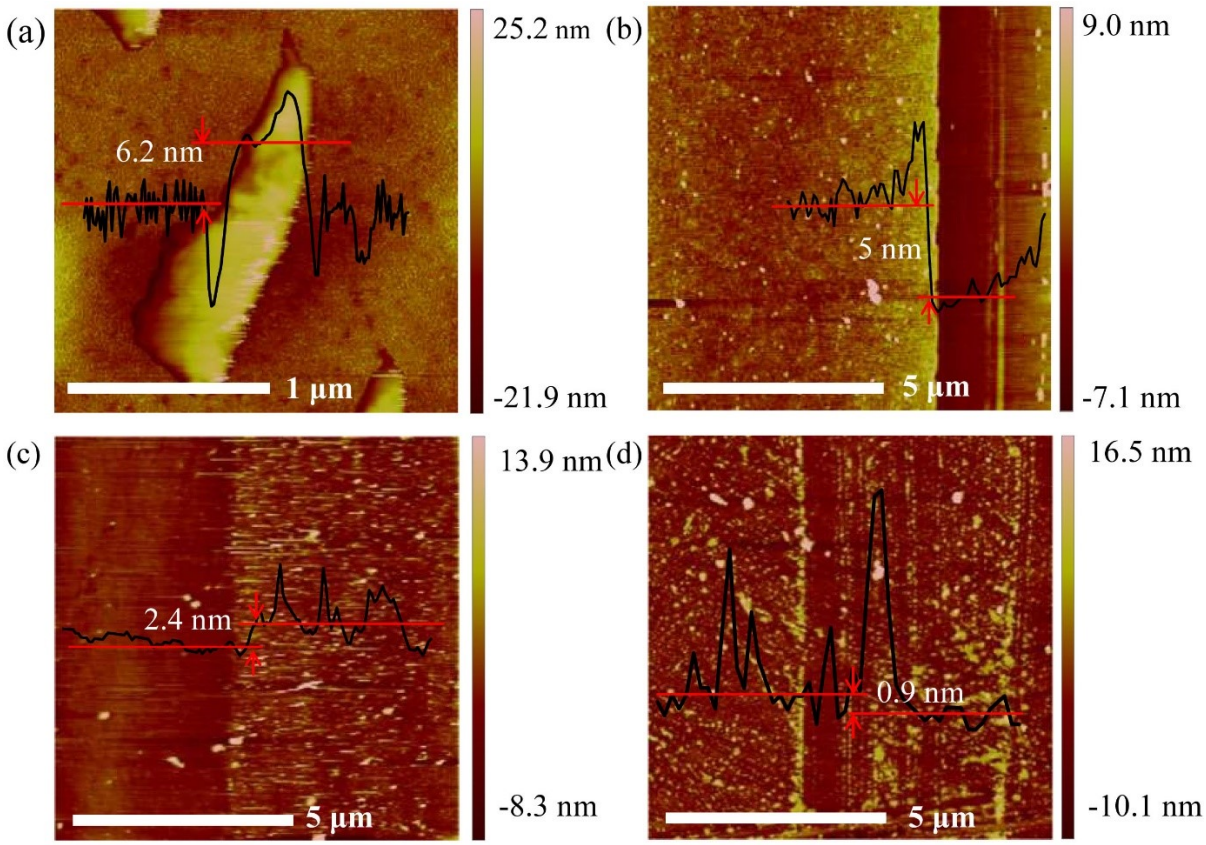

Figure S3. The AFM images of (a) LPE-MoS_2 nanosheets, CVD grown (b) 7L-, (c) 3L- and (d) 1L- MoS_2 films.

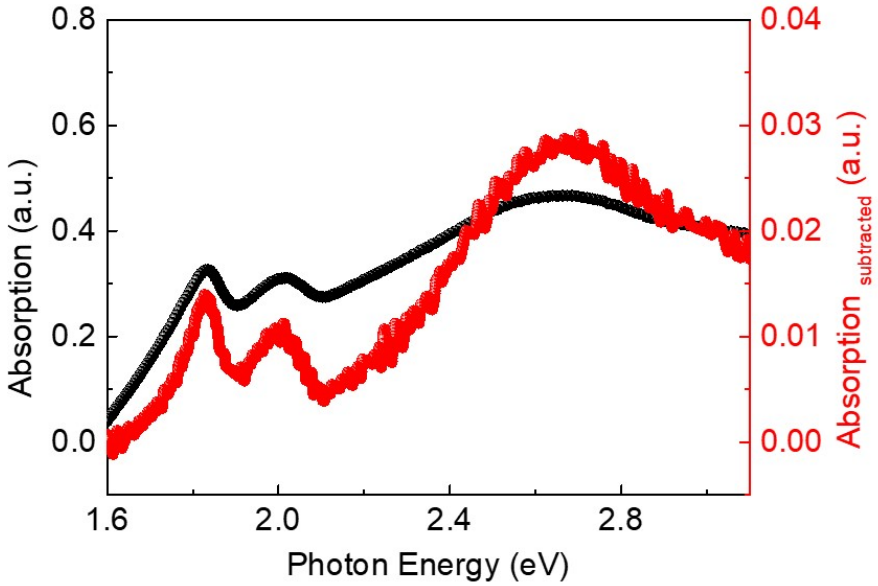

Figure S4. The absorption spectra before (black) and after (red) a background removal.

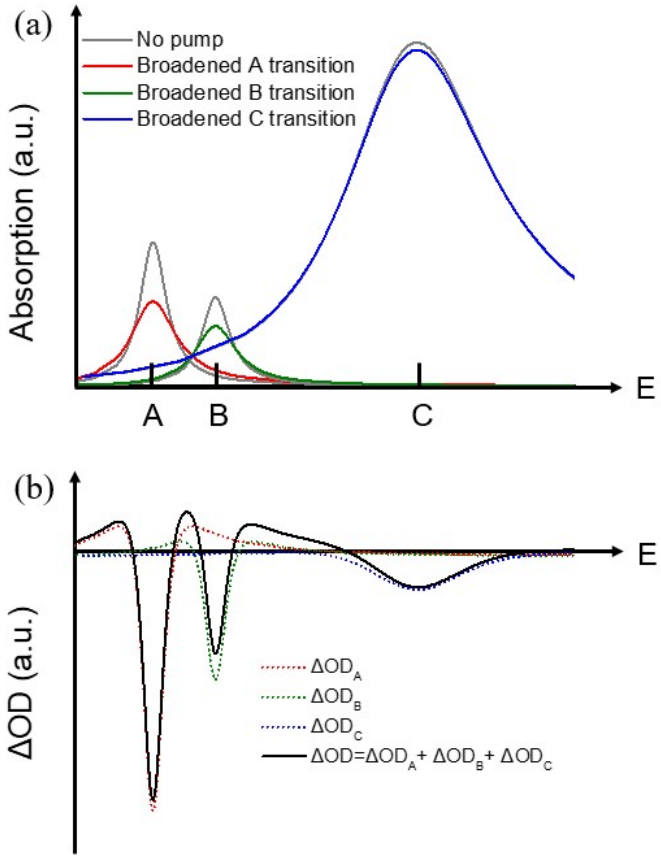

Figure S5. Schematic illustration for the spectral overlapping of exciton states in TA experiments. (a) Three Lorentzian functions corresponding to the exciton resonance peaks of X_A, X_B and X_C states without pump are shown in grey curves. After pump, those Lorentzian curves are broadened (color curves). (b) The TA spectra are fitted by adjusting the parameters (the linewidths) of those Lorentzian functions.

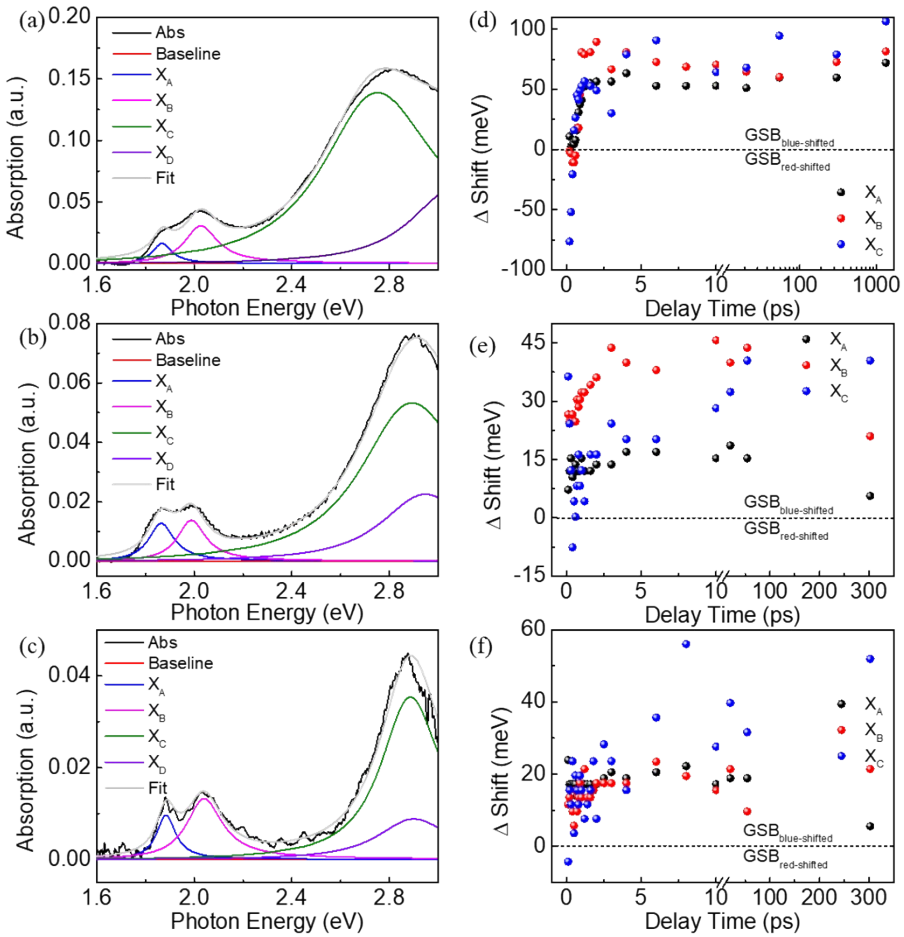

Figure S6. Multi-peak fitting for the steady-state absorption spectra (black line, its background has been subtracted) of CVD grown (a) 7L, (b) 3L and (c) 1L MoS_2 films by absorption Lorentzian functions. The peak shifting kinetics of X_A, X_B and X_C states as a function of delay time for CVD grown (d) 7L, (e) 3L and (f) 1L MoS_2 films.

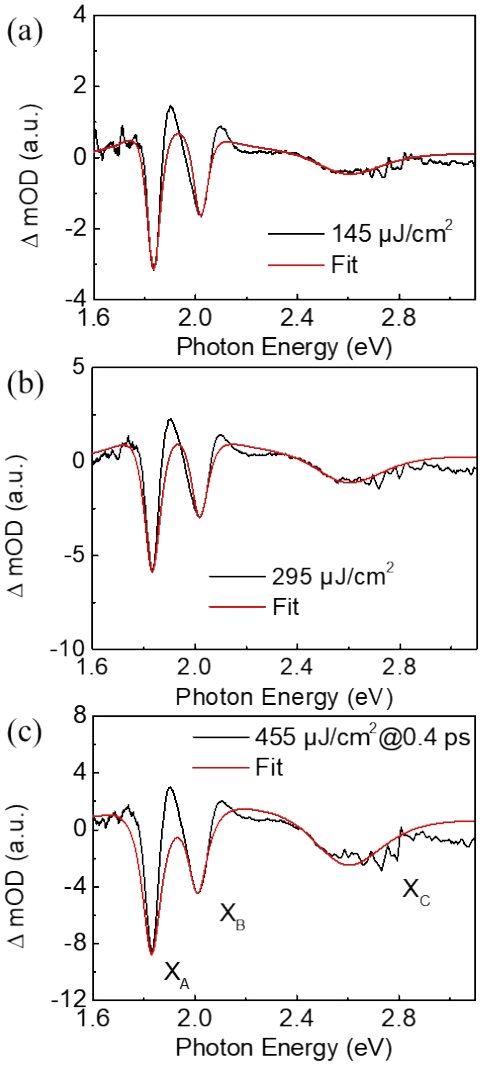

Figure S7. Peak broadening in LPE-MoS_2 nanosheets. TA spectra probed at initial delay times are fitted by summarizing the differential spectra of absorption Lorentzian with only varying peak widths for all the three exciton states under 400 nm excitation with the pump density of (a) 145, (b) 295 and (c) 455 μJ/cm^2, respectively. At the pump density of 455 μJ/cm^2, the fitted curve has already presented obvious deviations in comparison with the initial TA spectrum, even for the GBS peak of X_A. At a larger pump density condition, like 885 μJ/cm^2, this fitting method does not work, since the deviations are too large to accept for fitting the inital TA spectrum by only considering peak broadening effect. This could be due to that for high pump density conditions, the other quasiparticles including trions (like X_A^-) and charges (like C-charges) are also responsible for the initial TA spectrum of LPE-MoS_2 nanosheets as shown in Figure 4a.

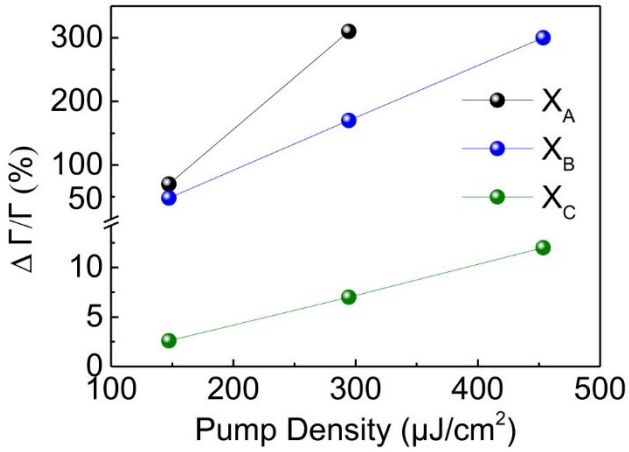

Figure S8. Peak broadening of X_A, X_B and X_C states as a function of pump density at the initial decay time (maximum values).

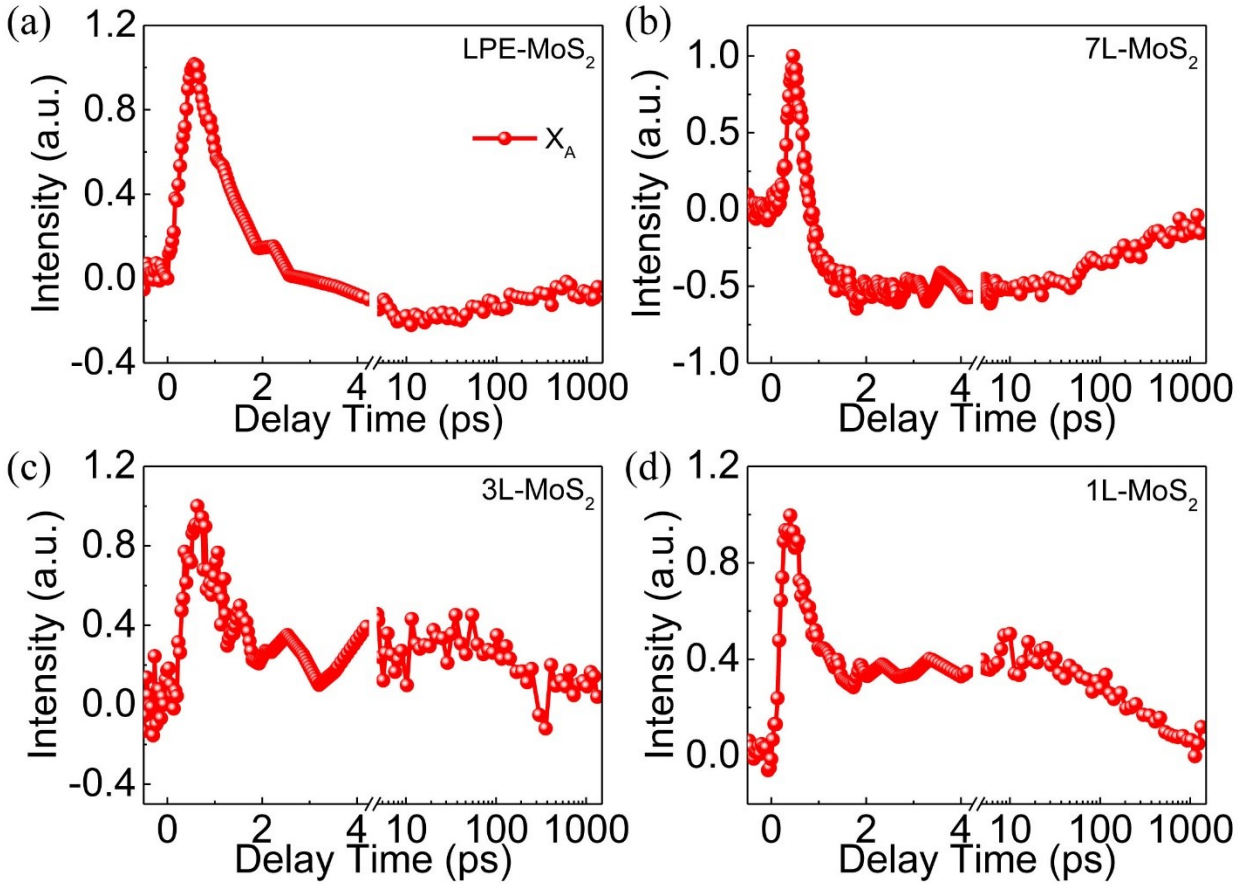

Figure S9. Normalized dynamics of X_A states under relatively low pump densities for (a) LPE-MoS_2 nanosheets, CVD grown (b) 7L-, (c) 3L- and (d) 1L-MoS_2 films. Due to the overlapping between the negative GSB signals and large positive signals at the X_A states of LPE-MoS_2 nanosheets and CVD grown 7L-MoS_2 films, it is hard to fit a satisfactory result for the corresponding X_A dynamics. It is the same reason that we cannot fit the X_A dynamics of all samples under relatively high pump densities.

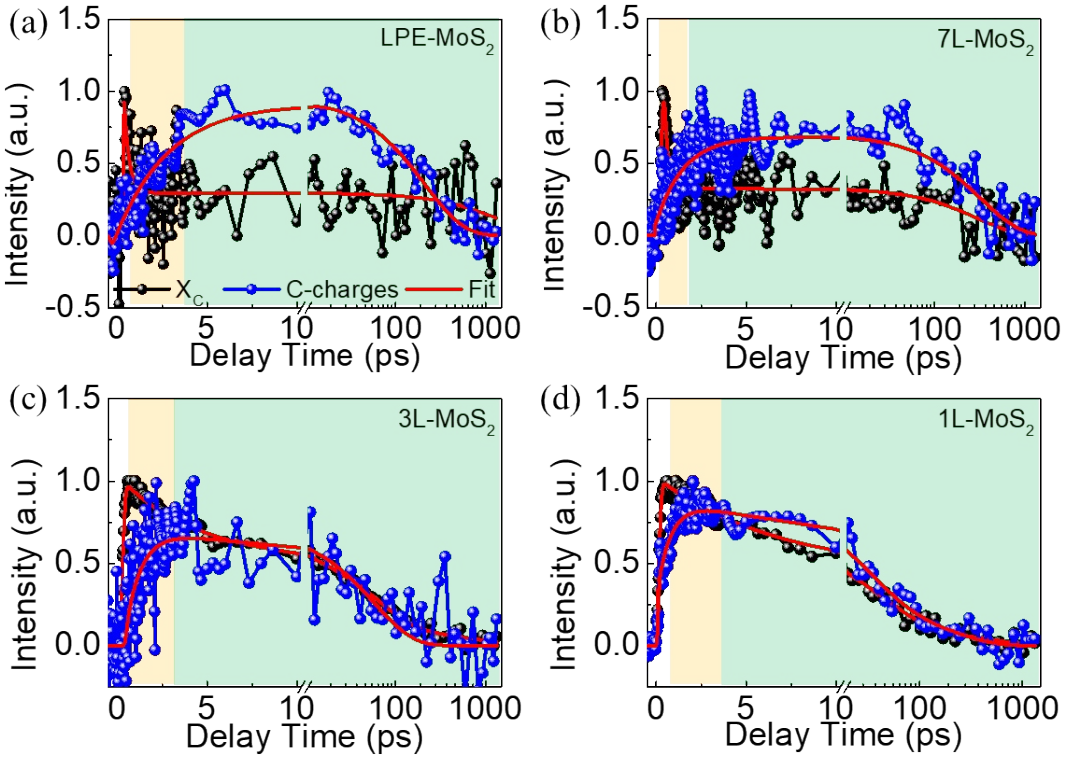

Figure S10. Normalized dynamics of X_C and C-charge states under relatively low pump densities for (a) LPE-MoS_2 nanosheets, CVD grown (b) 7L-, (c) 3L- and (d) 1L-MoS_2 films.

Table S1. Exciton binding energy of LPE-MoS_2 nanosheets, CVD grown 7L, 3L and 1L MoS_2 films.

	X_A (meV)	X_B (meV)	X_C (meV)
LPE-MoS_2	77	76	-70
7L-MoS_2	60	70	-76
3L-MoS_2	20	44	-8
1L-MoS_2	22	20	-4

Table S2. Best−Fit Parameters of Peak Broadening for X_A, X_B and X_C States in MoS_2 Nanosheets by a Multi-Exponential Function, $I(t) \propto \Sigma_i A_i \exp(-t/\tau_i)$, at a Pump Density of 145 $\mu J/cm^2$ in Figure 3.

Probe	$\tau_{\text{decay 1}}$ (ps)	$\tau_{\text{decay 2}}$ (ps)
X_A	0.39±0.02 (92%)	2140±107 (8%)
X_B	0.57±0.02 (88%)	1460±73 (12%)
X_C	0.13±0.01 (80%)	6580±329 (20%)

Table S3. Best−Fit Parameters of X_A^- States in MoS_2 Materials by a Multi-Exponential Function, $I(t) \propto \Sigma_i A_i \exp(-t/\tau_i)$, at a Relatively Low Pump Density in Figure 5.

Sample	Probe	$\tau_{arising}$ (ps)	$\tau_{decay\ 1}$ (ps)	$\tau_{decay\ 2}$ (ps)	$\tau_{decay\text{-}avg}$ (ps)
MoS_2 nanosheets	X_A^-	0.24±0.01	0.87±0.04 (69%)	607±30 (31%)	189
7L-MoS_2	X_A^-	0.69±0.03	280±14	-	280
3L-MoS_2	X_A^-	0.66±0.03	22±1.1	-	22
1L-MoS_2	X_A^-	0.48±0.02	38±1.9	-	38

Table S4. Best−Fit Parameters of X_C and C-Charge States in MoS_2 Materials by a Multi-Exponential Function, $I(t) \propto \Sigma_i A_i \exp(-t/\tau_i)$, at a Relatively Low Pump Density in Figure S10.

Sample	Probe	$\tau_{arising}$ (ps)	$\tau_{decay\ 1}$ (ps)	$\tau_{decay\ 2}$ (ps)	$\tau_{decay\ 3}$ (ps)	$\tau_{decay\text{-}avg}$ (ps)
MoS_2 nanosheets	X_C	-	0.29±0.01 (69%)	1483±74 (31%)	-	460
	C-charge	3.09±0.15	213±10	-	-	213
7L-MoS_2	X_C	-	0.12±0.01 (87%)	295±15 (13%)	-	38
	C-charge	1.58±0.08	324±16	-	-	324
3L-MoS_2	X_C	-	3.80±0.19 (40%)	62±3.1 (50%)	829±41 (10%)	115
	C-charge	0.87±0.04	58±2.9	-	-	58
1L-MoS_2	X_C	-	5.38±0.27 (40%)	47±2.4 (50%)	469±23 (10%)	73
	C-charge	0.76±0.04	32±1.6 (71%)	194±10 (29%)	-	79

Table S5. Best−Fit Parameters of X_C and C-Charge States in MoS_2 Materials by a Multi-Exponential Function, $I(t) \propto \Sigma_i A_i \exp(-t/\tau_i)$, at a Relatively High Pump Density in Figure 6.

Sample	Probe	$\tau_{arising}$ (ps)	$\tau_{decay\ 1}$ (ps)	$\tau_{decay\ 2}$ (ps)	$\tau_{decay\ 3}$ (ps)	$\tau_{decay\text{-}avg}$ (ps)
MoS_2 nanosheets	X_C	-	1.34±0.07 (52%)	7.86±0.39 (17%)	3335±167 (31%)	1036
	C-charge	1.85±0.05	116±5.8 (37%)	568±28 (63%)	-	400
7L-MoS_2	X_C	-	0.31±0.005 (62%)	19±0.8 (13%)	450±15 (25%)	115
	C-charge	0.45±0.01	179±9 (49%)	512±26 (51%)	-	349
3L-MoS_2	X_C	-	1.02±0.05 (27%)	109±4.4 (64%)	1483±74 (9%)	204
	C-charge	1.21±0.05	127±6.3 (94%)	2077±104 (6%)	-	244
1L-MoS_2	X_C	-	1.96±0.10 (28%)	74±3.3 (72%)	-	54
	C-charge	1.34±0.07	79±4.0	-	-	79